American Journal of Computational Mathematics, 2025, 15(2), 209-218
https://www.scirp.org/journal/ajcm
ISSN Online: 2161-1211
ISSN Print: 2161-1203

Applying Conformal Mapping to Determine the Electric Field of a Non-Concentric Cylindrical Capacitor and Its Capacitance

Haiduke Sarafian

University College, The Pennsylvania State University, York, USA
Email: has2@psu.edu

How to cite this paper: Sarafian, H. (2025) Applying Conformal Mapping to Determine the Electric Field of a Non-Concentric Cylindrical Capacitor and Its Capacitance. *American Journal of Computational Mathematics*, **15**, 209-218.
https://doi.org/10.4236/ajcm.2025.152011

Received: May 27, 2025
Accepted: June 27, 2025
Published: June 30, 2025

Abstract

A cylindrical capacitor's electric field of non-concentric double circular shells is determined and graphed by applying conformal mapping. It is demonstrated, using the Computer Algebra System (CAS) *Mathematica*, primarily numerically, how the lack of symmetry in the configuration is addressed and handled. Numerically, various essential properties of the applied conformal transformation are investigated. This article examines the relationship between the associated capacitance and the separation distance between the centers of the shells. It reveals its unexpected, peculiar behavior at a certain separation distance between the shells. Numerous quantities of interest are graphed visually in the mentioned electric field between the shells, enhancing the understanding of the issues at hand. The article embodies *Mathematica* codes, enabling their reproduction and enriching and deepening the field of interest.

Keywords

Conformal Mapping, Electric Field of an Asymmetric Double-Shell Capacitor, Capacitance of an Asymmetric Double-Shell Capacitor, Computer Algebra System, *Mathematica*

1. Introduction

Figure 1 displays the pictorial foundation of this investigation. Its left panel shows two different-sized nonconcentric "infinitely" long parallel cylindrical shells. Assuming the smaller-sized shell is charged positively, with a charge +q colored red on its surface, the larger one is charged negatively, having a charge −q colored blue on its surface. The structure carries a net charge of zero. Figure 1 depicts the profile of a generalized configuration of a classic cylindrical capacitor.

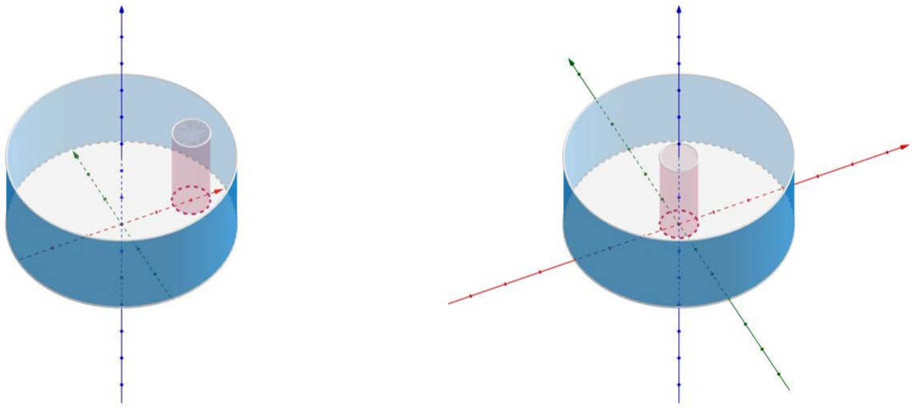

Figure 1. 3D views of the cylindrical capacitor. The left frame depicts the issue at hand, and the right frame has a traditional symmetric configuration.

Noting that, depending on the objective of the investigation, one may assign potential to the shells. A positive potential voltage, $+V_0$, can be assigned to the inner shell, and a negative voltage, $-V_0$, to the outer shell, respectively, or vice versa; resulting in $|\Delta V| = 2V_0$.

This investigation has various objectives. Different criteria have been used in multiple subsections of the Formulation Section.

According to the left-side panel of **Figure 1**, one may be curious about the electric field configuration in the region between the shells for a charged capacitor. If one poses the same question to the right-side panel of **Figure 1**, the answer would be evident because of the symmetric configuration [1]. Bringing to the fore that, as a general known "rule", asymmetric configurations usually embody challenges. As such, the lack of a symmetric configuration, as shown in the left panel of **Figure 1**, presents challenges. These challenges are addressed in the forthcoming paragraphs. Hence, the first objective is to quantify and display the electric field mentioned. The second auxiliary objective is to determine the capacitance of the shown capacitor.

The complex potential methodology has been adapted to fulfill our objectives, especially its affiliated *conformal mapping*. The application of this method to the problem at hand is discussed in detail in the forthcoming sections. **Figure 2** pictorially shows the essence of this approach. In short, two complex planes are shown, the z-plane and the w-plane. The z-plane deals with the asymmetric configuration, while the w-plane is its symmetric version after conformal mapping. As pointed out earlier, solving the issue in the w-plane is trivial, so the information obtained through an inverse transformation can be identified as the solution to the actual problem.

Adapting this method has posed challenging issues. Literature has either ignored or left these challenges unanswered. So, this article may be viewed as a contribution to the field. Its CAS accompaniment makes it suitable for computational physics and mathematics.

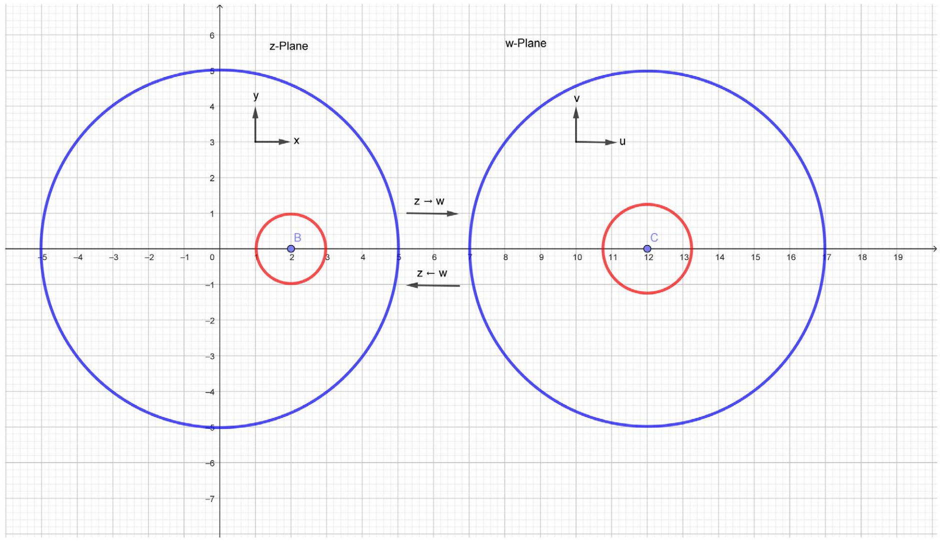

Figure 2. These are the 2D one-to-one profiles of the corresponding Figure 2.

Furthermore, it is known that, according to conformal mapping, a circle in the z-plane is mapped onto itself; however, literature does not provide information on its realizability. The latter has a severe impact on calculating capacitance. In this article, we address this issue graphically, showing the size of the resized or transferred circle. Because the information is based on the separation distance between the centers of the circles or cylinders, we have identified a distance that is conducive to an unexpected character, which undermines the local minimum of a quantity of interest. This feature is discussed in the forthcoming paragraph.

One more point. Figure 1 and Figure 2 show only two static frames out of many animated running frames! For both cases, the inner cylinder in Figure 1 and its circular top or bottom views in Figure 2 in the draft version show the movement of the inner cylinder and its accompanying circles in Figure 2. Avoiding clothing, the article only includes two frames. And hence, the animation mode is tied to the quantity of interest. This means that while the animation is active, the interest also gets animated. These features are not included due to the journal's page limitation mandate.

This passage describes the general objectives and is systematically organized as follows:

The second section presents the problem formulation, along with the introduction. This section highlights the application of Conformal Mapping, specifically the format of the electric field as a function of the separation distance between the centers of the cylinders. This section also evaluates the capacitance of the capacitor mentioned. The article contains numerous CAS and *Mathematica* [2] codes, which code the reproduction of a leaning vehicle.

Several ideas were proposed throughout the presentation to produce fresh, publishable articles. The interested reader may wish to consider the challenges of publishing under their name. Section 3 is the Conclusion and remakes, finishing the article with References.

2. Formulations and Analysis

2.1. Few Words about Conformal Mapping

In this section, we begin with the fundamentals of conformal mapping. To be specific, consider the left panel of **Figure 2**, which depicts the top view of the cylindrical shells and the circles. The configuration shown lacks symmetry; the circles are not concentric. Assigning positive and negative potential to the circles makes it challenging to determine the potential in the region between the circles. The potential is needed to determine the electric field, according to the boundary's specifications, as referred to in the Introduction. The potential Φ is subject to the homogeneous Laplace equation, $\nabla^2\Phi = 0$. More specifically, in the z-plane with coordinates (x, y), the latter reads,

$$\left(\frac{\partial^2}{\partial x^2}+\frac{\partial^2}{\partial y^2}\right)\Phi(x,y)=0, \tag{1}$$

One way to "simplify" the problem is to transfer the configuration to another plane, a w-plane with coordinates (u,v) with a symmetrized configuration; concentric circles are shown on the right panel of **Figure 2**. This is utilizing a specific transforming *analytic* function, $w = f(z) = u(x,y) + \mathrm{i}v(x,y)$ Inheriting the Cauchy-Riemann property [3],

$$\frac{\partial u}{\partial x}=\frac{\partial v}{\partial y},\frac{\partial u}{\partial y}=-\frac{\partial v}{\partial x}, \tag{2}$$

$$\left(\frac{\partial^2}{\partial x^2}+\frac{\partial^2}{\partial y^2}\right)\Phi(x,y)=\left|f'(z)\right|^2\left(\frac{\partial^2}{\partial u^2}+\frac{\partial^2}{\partial v^2}\right)\Phi(u,v), \tag{3}$$

Φ stays invariant under the transformation between the z-plane and the w-plane. Assuming $f'(z) \neq 0$ (1) yields the right-hand side of (3), which is the Laplace equation for $\phi(u,v)$. Thus, the Laplace equation sustains its integrity.

Taking this as a short "known" review, we now consider a $w = f(z)$ Conformal transformation. We select a transformation from the "encyclopedia" [4], and [5] [6]. This is a *bilinear fractional* function, with only one parameter, *α*.

$$f_\alpha(x,y)=\frac{z-\alpha}{1-\alpha z}, \tag{4}$$

First, (4) satisfies the criteria. $f'(z) \neq 0$. Being a *conformal*, it preserves the angle between two intersecting curves, e.g., the horizontal axis and the circular curve in the z-plane, *i.e.*, a π/2 angle. Being a bilinear transformation, it *slides* the shapes between the z-plane and the w-plane so that a circle remains a circle before and after the transformation.

More specifically, (4) is formatted such that a unit circle, *i.e.*, a circle with a unit radius, transforms into a unit circle. This is not true for any other circle; the transformed circles are resized. In the upcoming section, we will show that the resized radii depend on the separation distance between the circles in the z-plane. The latter two features are depicted in **Figure 2**.

Because one objective of this note is to optimize the usage of the Computer

Algebra System (CAS), Mathematica, we craft a code that features this transformation.

2.2. Calculation

We begin with the fundamentals. Writing the left-hand side of (4) as $u(x,y)+\mathrm{i}v(x,y)$ and replacing its z variable with $z=x+\mathrm{i}y$ yields,

$$\begin{cases} u(x,y)=\dfrac{1}{D(x,y)}\left(\left[(x-\alpha)(1-\alpha x)-\alpha y^2\right]\right) \\ v(x,y)=\dfrac{y}{D(x,y)}\left[(x-\alpha)\alpha+(1-\alpha x)\right] \end{cases}, \tag{5}$$

where the denominator is $D(x,y)=(1-\alpha x)^2+\alpha^2y^2$.

To determine the value of α, consider a circle of radius. $\frac{1}{2}\left(\frac{1}{2}-\frac{1}{7}\right)=0.178$. Centered at 9/28 = 0.32 units in the z-plane. Where 1/2 and 1/7 are the abscissa of the right and left edges of the small circle depicted in **Figure 2**. Solving the equality, $f_\alpha\left(\frac{1}{7}\right)=-f_\alpha\left(\frac{1}{2}\right)$ yields a quadratic equation with two roots, $\alpha = 3$ and 1/3. Selecting the lesser than unity root, 1/3, transfers the circle onto a centered circle of radius. $f_{\frac{1}{3}}\left(\frac{1}{2}\right)=\frac{1}{5}=0.2$. This indicates that the radius of the transferred centered circle is enlarged by 12%, as shown in the w-plane in **Figure 2**.

Now it is straight forward to solve Laplace's equation, Equation (1) in the w-plane,

$$\left(\frac{\partial^2}{\partial u^2}+\frac{\partial^2}{\partial v^2}\right)\Phi(u,v)=0, \tag{6}$$

Because of the symmetry of the configuration shown on the right-hand panel of **Figure 2**, it is efficient if (6) is transferred into the cylindrical coordinate system, (r,φ,z). Its radial term is,

$$\left(\frac{\partial^2}{\partial r^2}+\frac{1}{r}\frac{\partial}{\partial r}\right)\Phi(r)=0, \tag{7}$$

With a solution, $\Phi(r)=A\ln r+B$ where $r=\sqrt{u^2+v^2}$. The coefficients A and B can be determined by assigning potentials to the inner and the outer circles. With the variables of the w-plane. Equation (7) yields,

$$\Phi(u,v)=\frac{A}{2}\ln\left(u^2+v^2\right)+B, \tag{8}$$

And since the objective is to determine the potential in the z-plane, the u and v should be substituted utilizing (5). The corresponding *Mathematica* codes [7] [8] are:

```
den[x_,y_]=(1-α x)²+(α y)²/.α->1/3;
u[x_,y_]=1/den[x,y] ((x-α)(1-α x)-α y²)/.α->1/3;
v[x_,y_]=y/den[x,y] ((α(x-α)+(1-α x)))/.α->1/3;
ϕ[x_,y_]=-(1/2) Log[u[x,y]²+v[x,y]²]-1;
(*voltage of the inner circle is set at +1 and the outer at −1. The log has a factor
```

of 1.15, but the argument of the log is Sqrt[u^2+v^2], which gives another factor 1/2, making the overall factor 1.15/2*)

Utilizing the potential, the electric field is given by $\mathbf{E} = -\nabla\Phi(x, y)$. In other words, grad $\phi(x, y)$

$$\text{grad} = -\text{Grad}\left[\phi[x, y], \{x, y\}\right];$$

The latter is displayed using the **StremPlot** command, as shown in Figure 3.

plot0=StreamPlot[Evaluate[+Grad[x²+y²,{x,y}]],{x,-1,1},{y,-1,1},RegionFunction->Function[{x,y},(x)^2+y^2>0.2²&&x^2+y^2<1.],Axes->True,StreamStyle->Black];

And finally, putting all these pieces together, we display the final aimed result,

contourPlot=ContourPlot[ϕ[x,y],{x,-1,1},{y,-1,1},ContourShading→Fals(*ImageSize->Large*),Contours->20,RegionFunction->Function[{x,y},(x-0.32)^2+y^2>0.2²&&x^2+y^2<1.]];

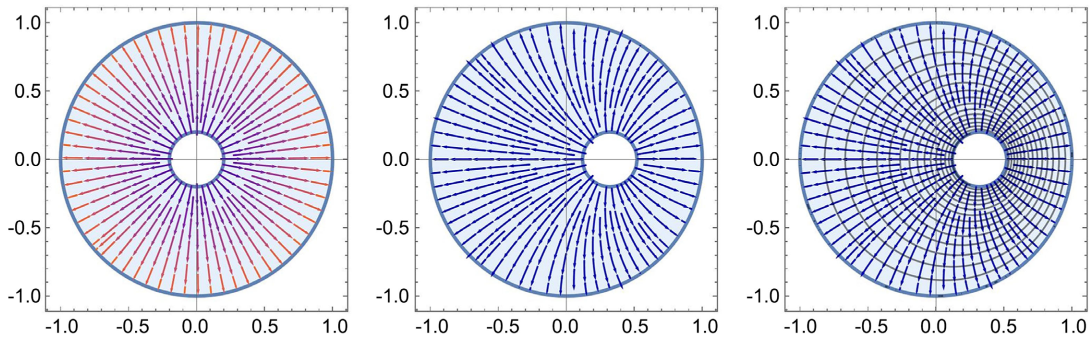

Figure 3. From left to right, 2D configuration profiles of cylindrical configuration and associated electric field co-centric, off-centered, and off-centered contours and E-fields, respectively.

2.3. More on Conformal Mapping

Equation (4) is the transformation function between the z-plane and the w-plane. Table 1 illustrates the transformation of coordinates and specific points.

Table 1. Four points selected on the z-plane, the first column, are transferred to associated points in the w-plane, the second column, according to (4). The last column shows that a unit circle in the z-plane remains a unit circle in the w-plane.

Points in z-plane	→	Points in w-plane	Output in w-plane
1	→	1	
−1	→	−1	
i	→	$\begin{cases} u = -\dfrac{2\alpha}{1+\alpha^2} \\ v = \dfrac{1-\alpha^2}{1+\alpha^2} \end{cases} \rightarrow$	$u^2 + v^2 = 1$
-i	→	$\begin{cases} u = -\dfrac{2\alpha}{1+\alpha^2} \\ v = -\dfrac{1-\alpha^2}{1+\alpha^2} \end{cases} \rightarrow$	$u^2 + v^2 = 1$

The first two rows of the table show that points on the x-axis of the z-plane are transformed to identical points on the u-axis of the w-plane. The 3rd and the 4th rows show the transformed coordinates of the y-axis on the z-plane to a pair of symmetric complex points on the w-plane; these points are α-dependent. The corresponding 3rd and 4th columns justify the equal unity modules of these points. In other words, the conformal mapping function (4) transforms a unit circle in the z-plane to a unit circle in the w-plane.

Nonetheless, from a programming point of view, the author faced a necessary challenge in crafting a subprogram that displays the applicability of the features of Table 1 for all points on the unit circle, as well as the smaller circle in the z-plane and its transformed, enlarged circle in the w-plane. Due to the length of the code, it is skipped; however, its graphical output is shown in Figure 4.

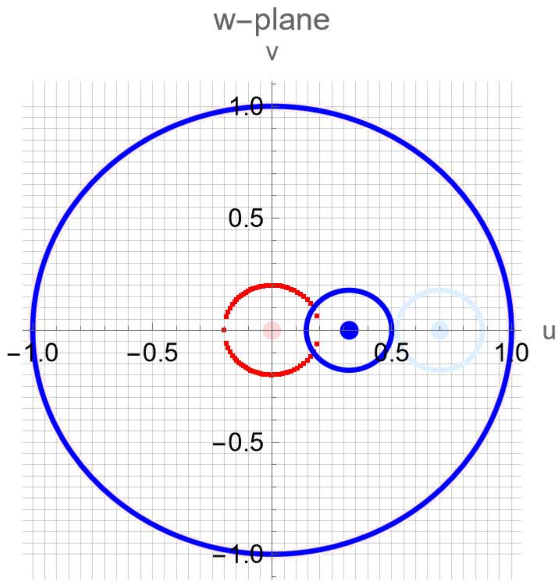

Figure 4. The solid blue curves are the original unit and the small circles in the z-plane, respectively. The thick pink curve and the dotted red points are the corresponding conformal transferred circles in the w-plane.

The far end light blue circle shows the image of the displayed circle that is slid further. This one, too, after being transformed into the w-plane, became the red dotted circle shown.

2.4. Capacitance

In conjunction with the problem at hand, a curious question is, what is the capacitance of the nonconcentric capacitor? In the case of a parallel-plate capacitor, the capacitance changes in proportion to the distance between the plates. Specifically, according to a trivially proven formulation and the symmetry of the electric field between the parallel plates for a fixed plate area A, the capacitance is $C = \epsilon_0 A/d$. Where A is the common exposed surface area of the plates. The issue concerning the cylindrical capacitor at hand is not too trivial. This is because by sliding the inner shell/circle "closer" to the outer shell, the distance to the opposite side "increases" although the common exposed surface area stays unchanged. One way to resolve the issue is to utilize the well-known information for a concentric double-shell capacitor. Here again, due to the symmetry of the electric field between the shells, it can be proven [2] $C/\epsilon_0 (2\pi\ell)q = \left[\ln\left(\frac{r_2}{r_1}\right)\right]^{-1}$. Here is the point: by applying the practiced conformal mapping in the w-plane, the off-centered shells are transformed into a concentric shell. Making the latter formulation applicable. As mentioned previously, we intentionally utilized a unit circle, and as shown in **Figure 2**, according to the practiced conformal mapping, the unit circle remains a unit circle after transformation. But any other circle acquires an enlarged size. Putting this fact in action, r_1 labels the radius of the small ring, and r_2 labels unity, the radius of the unit circle. In short, the RHS of the latter expression in the text, *i.e.*, the capacitance per charge and unit length, becomes the inverse logarithm of the radius in the w-plane. Therefore, the task is to evaluate the distance between the center of the shells and subtract this distance from the units to obtain the distance between the surface of the shells and the outer cylinder's surface. This requires a multistep process. 1) Although in the z-plane, the inner shell, by sustaining its radius, slides toward the outer shell, its center changes the distance, affecting the α parameter of the transformation. 2) Evaluation of the mentioned α assists in determining the radius of the centered circle in the w-plane, r_1.

The result of all these steps is shown in the graph (**Figure 5**).

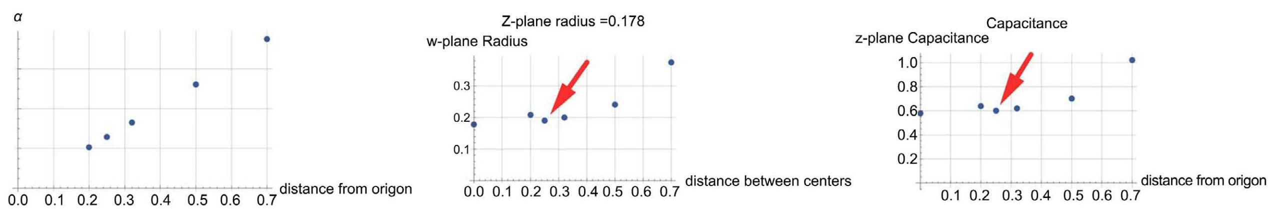

Figure 5. From left to right. All three graphs have the same horizontal axis label, "distance from the origin". The conformal parameter α, the radius of the circles in the w-plane, and the capacitance of the capacitor in the z-plane, respectively.

The far-left plate shows the linear character. Note, sliding the original small circle along the x-axis in the z-plane requires the determination of a unique α. The abscissa of the coordinate shown in the picture shows that the circle is moved from 0.2 to 0.7 units five times. The second panel of the exact figure displays the resized radius and enlarged radius of the small circle in the w-plane. The α's depicted on the left panel are used in crafting this diagram. The graph's title displays the circle's original radius, 0.178 units in the z-plane. The third panel displays the capacitance of the original asymmetric cylindrical capacitor as a function of the coordinate location of the smaller circle or cylinder.

The right panel of Figure6 displays the capacitance of the capacitor at hand and the variation of its values as a function of the coordinate/position relative to its center from the wall of the unit circle. This graph is designed for comparison with the standard characteristics of a parallel-plate capacitor. As such, by adjusting the separation between the plates of the latter according to the expression given in the last paragraph, the most significant separation between the plates results in the lowest capacitance. This feature is "almost" true for the cylindrical capacitor at hand. A red arrow indicates an exceptional separation distance as shown in **Figure 6**, and the second point is located at the far-right end of the second panel of **Figure 7**. This point displays a local maximum value. One might argue that this is a numerical error. The author believes this feature has a fundamental physical/mathematical origin. An analysis is currently underway to investigate the issue.

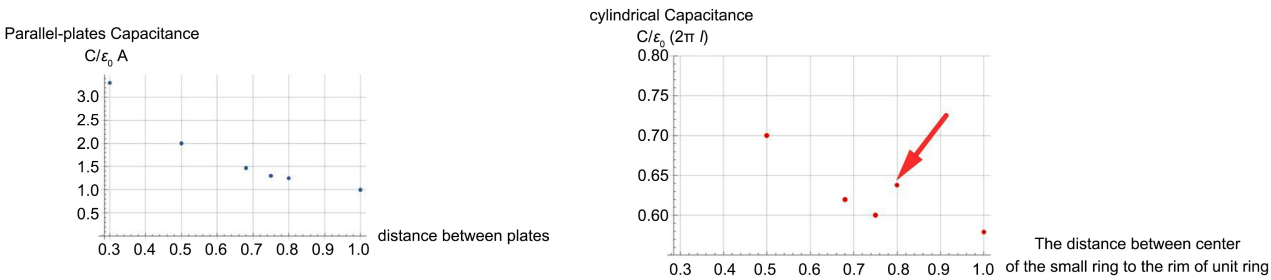

Figure 6. Both diagrams have the "same" axis labels. The first graph displays the normalized value of a parallel-plate capacitor, while the second graph shows the associated capacitance for the asymmetric cylindrical capacitor.

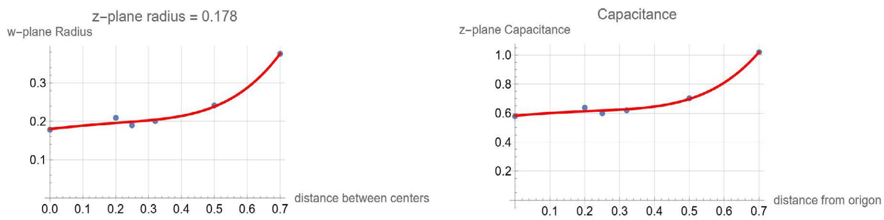

Figure 7. The original w-plane radii of the small circle, with a radius of 0.178 units, after transformation in the w-plane, versus the distance between the circles, areshown in **Figure 2**. The second plate is associated with the capacitance in the z-plane.

To fit the data, a continuous function is explored by trial and error. This curve helps determine the quantity of interest by bypassing the time-consuming repetition of calculations.

3. Conclusions and Summary

This multiple-faceted research-oriented note has numerous objectives. The foremost aim is to study the impact of a symmetrical broken configuration. A double-shell, infinitely long, parallel cylindrical capacitor with off-centered orientation is considered. Asymmetrical configuration introduces challenging mathematical and computational issues. Its computational aspect is successfully addressed utilizing a Computer Algebra System (CAS) such as *Mathematica*. Its mathematical elements are addressed by applying complex potential theory, particularly through the use of conformal mapping. Applying the latter, the asymmetric configuration in the complex z-plane was converted into a symmetric configuration in the w-plane. The outcome of formulating the issue in the w-plane is then transformed into the z-plane. Although the mentioned narrative sounds practical in theory, the author encountered numerous challenging and time-consuming programming issues that required resolution. The report embodies mostly numerically intensive graphic results. Almost all the programming codes are included to assist the interested reader in reproducing the results. The second main objective is to evaluate the capacitance of the capacitor at hand. Not only has the value been calculated for one specific configuration, but the animation of the configuration for different scenarios conducive to variation of the calculated capacitors is determined and graphed accordingly.

During the numerical analysis of capacitance, a specific configuration is identified that locally maximizes the capacitance. This is a curious result compared to a parallel-plate capacitor, which exhibits, intuitively, the expected behaviors. This feature would have remained undetected if the numeric analyses had labeled a numeric error. An analysis is underway to identify the origin.

Interested readers may find [7]-[9] to be valuable resources for programming.

Conflicts of Interest

The author declares no conflicts of interest regarding the publication of this paper.

References

[1] Jackson, J.D. (1999) Classical Electrodynamics. 3rd Edition, Wiley.

[2] *Mathematica*^{R}V14.1. http://Wolfram.com

[3] Sokolnikoff, I.S. and Redheffer, R.M. (1966) Mathematics of Physics and Modern Engineering. 2nd Edition, McGraw-Hill.

[4] Kober, H. (1960) Dictionary of Conformal Mappings. Dover Publications.

[5] Schinzinger, R. and Laura, P.A.A. (2003) Conformal Mapping: Methods and Applications. Dover Publications.

[6] Asmar, M.H. and Grafakos, L. (2018) Complex Analysis with Applications. Springer.

[7] Wolfram, S. (2003) The Mathematica Book. 5th Edition, Cambridge University Publications.

[8] Sarafian, H. (2019) Mathematica Graphics Examples. 2nd Edition, Scientific Search Publishing.

[9] Sarafian, H. (2023) Haiduke Sarafian's Collective Articles 2020-2023. Scientific Research Search Publishing.